DFT Study on the Nucleophilic Addition Reaction of Water and Ammonia to the Thymine Radical Cation

Jiyoung Heo[†] and Nam Joon Kim*[,‡]

Division of Chemistry and Chemical Engineering, California Institute of Technology, Pasadena, California 91125, and Department of Chemistry, Chungbuk National University, Chungbuk 361-763, Korea

Received: May 4, 2007; In Final Form: June 18, 2007

The nucleophilic addition reactions of water and ammonia molecules toward the C5−C6 double bond of thymine radical cations were investigated using density functional theory. We predicted that the nucleophilic addition favored the C5-site of thymine radical cations, in contrast to the previous experimental observations in bulk solution where the addition product to the C6-site was dominant. Considering the molecular orbital factors, we estimated the relative reactivity of the C5- and C6-sites of thymine radical cations for the nucleophilic addition of ammonia. We found that the C5 was more reactive than the C6 for the small-size clusters of $Thy_1(NH_3)_n^+$, $n = 0-2$, in the gas phase and even in aqueous solution, though the difference in the reactivity between the two sites became smaller as the number of ammonia molecules increased. This variation of the reactivity was attributed to the electron density redistribution within the thymine radical cations induced by the ammonia molecules as a nucleophile. We suggest that the dominance of the C6-addition product in bulk solution is mainly due to the higher stability of the C6-addition product by solvation, rather than to the higher reactivity of the C6-site for the nucleophilic addition.

Introduction

Ionizing radiation on DNA causes mutagenic and carcinogenic effects in a mammalian cell.[1−3] In particular, the radical cations of DNA bases generated by the ionizing radiation initiate the alteration of the bases, which is one of the main types of cytotoxic DNA lesions.[1] Many studies have been devoted, therefore, to the radical cations of DNA bases and their reactions in solution, in the solid state, and even in the gas phase.[4−9] Among four DNA bases, the radical cation of thymine has been of great interest because of its high reactivity with other species in a cell. It should be noted that in quinine-sensitized photooxidation of purines and pyrimidines, only the pyrimidine radical cations formed photoproducts.[10]

Since Sevilla and co-workers[11,12] first showed that thymine radical cations (Thy^+) can be produced by UV irradiation of thymine at 77 K in both alkaline and acidic glasses, their reactions have been extensively studied in the past decades[10,12−14] using electron spin resonance (ESR), electron paramagnetic resonance/electron nuclear double resonance (EPR/ENDO),[15] transient absorption,[16] and time-resolved Fourier transform electron paramagnetic resonance (FT-EPR).[17]

In those studies, the dominant reaction of Thy^+ in aqueous solution was found to be the deprotonation of N1. However, it was also observed that the nucleophilic addition reaction of water occurred on the C5−C6 double bond of Thy^+.

Sevilla and Engelhardt[18] reported the conversion of pyrimidine radical cations to the corresponding C6−OH adduct radicals by ESR in aqueous glasses. Shaw et al.[19] identified 6-hydroxy-5,6-dihydrothymidine isomers as a product of the hydration upon γ-irradiation of thymidine in frozen aqueous solution. The radical cations of N1-substituted thymine derivatives were proposed to decay by the water addition at C6 as well as the deprotonation from N3 or C5 methyl group in a pulse radiolysis

SCHEME 1

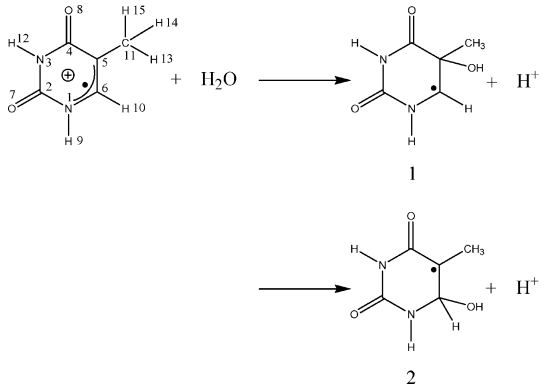

SCHEME 2

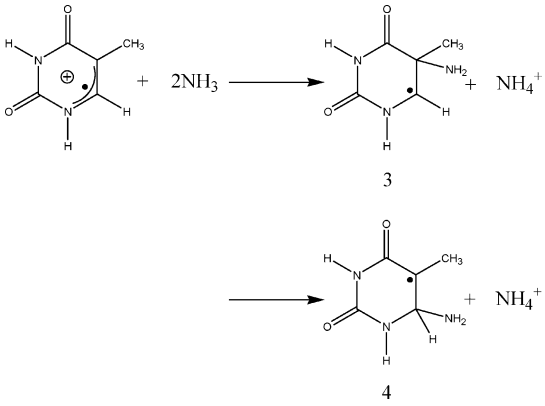

* Corresponding author. E-mail: namjkim@chungbuk.ac.kr.
[†] California Institute of Technology.
[‡] Chungbuk National University.

10.1021/jp0734124 CCC: $37.00
Published on Web 08/21/2007

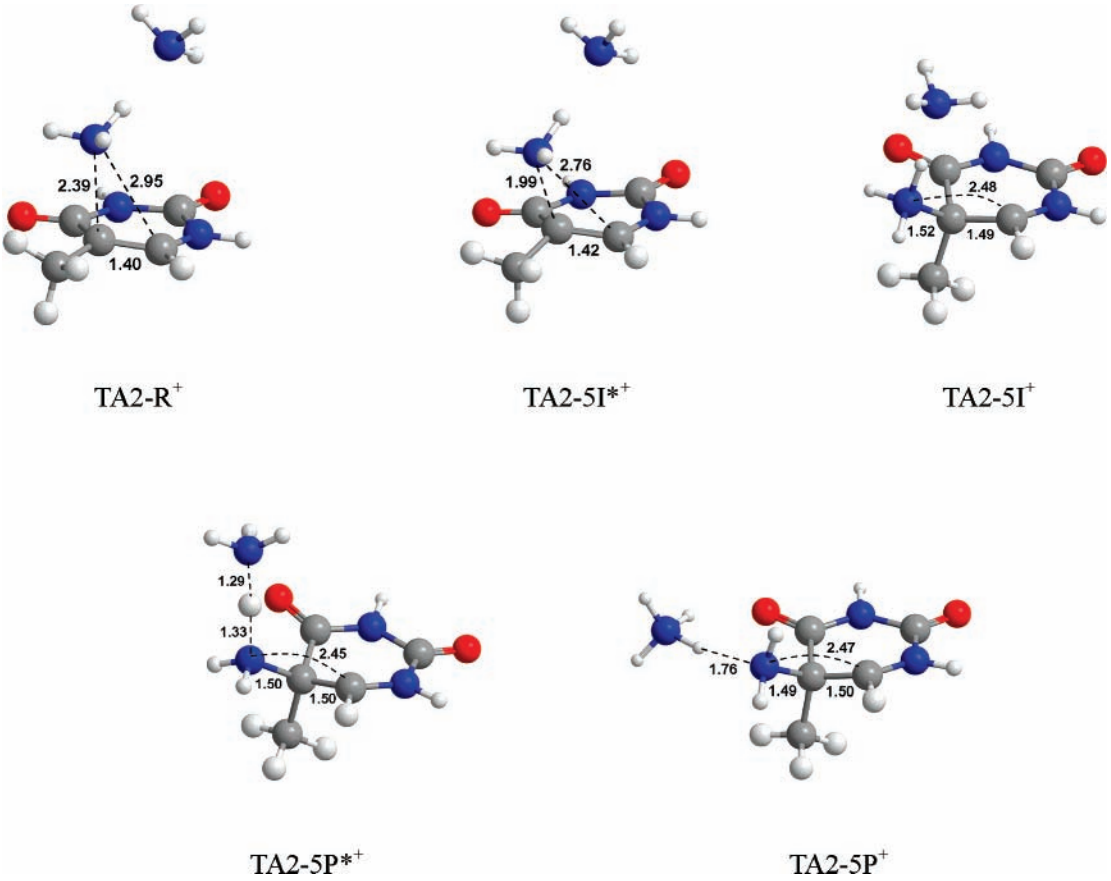

Figure 1. Optimized structures of solvated thymine radical cations with two ammonia molecules at the local minima or transition states along the reaction coordinate of the nucleophilic addition to the C5-site of Thy^+. The structures were fully optimized at the B3LYP/6-311++G(d,p) level.

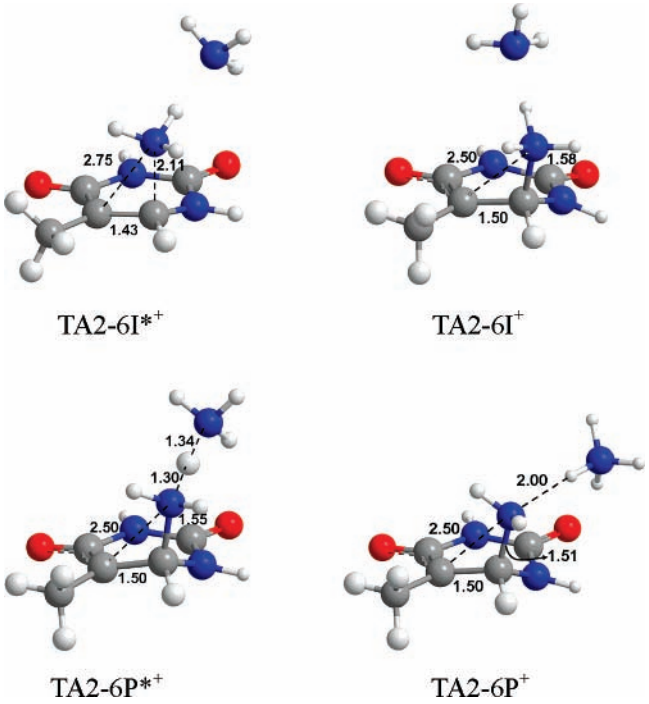

Figure 2. Optimized structures of solvated thymine radical cations with two ammonia molecules at the local minima or transition states along the reaction coordinate of the nucleophilic addition to the C6-site of Thy^+.

study with optical and conductance detection.[14] They also speculated that the water addition reaction would become more important in DNA where the N1 of thymine is substituted by the sugar moiety and the N3 is linked to the N6 of deoxyadenosine by a hydrogen bond so that the deprotonation channels of thymine radical cations are completely or partially blocked.[14] Wagner et al.[10] suggested from the distribution of products that the dominant reaction of thymine and thymidine radical cations generated by photosensitization was the water addition to give C6−OH adduct radicals. The generation of the C6−OH adduct radicals with a trace of the C5−OH from the water addition of the radical cations of 1-methylthymine was reported using FT-EPR.[20]

In those studies, the water addition to the C6-site was observed to be more favorable than that to the C5-site of Thy^+ in bulk solution. Interestingly, however, from the theoretical calculations described in this paper, we found that the C5-site was preferred for the nucleophilic addition to the C6-site in the thymine radical cation solvated with a few water or ammonia molecules, in contrast to the experimental observations. These contradictory results were explained here by estimating the relative reactivity of the C5 and C6 of Thy^+ toward the nucleophilic addition reaction and also the relative energies of the intermediate and transition states along the reactions of the C5- and C6-addition in the gas phase and in aqueous solution.

Computational Methods

The structures of local minima and transition states were fully optimized using density functional theory (DFT) employing a hybrid functional of B3LYP with a standard 6-31G(d) basis set. With the use of these optimized structures as starting geometries, the full optimizations at the B3LYP/6-311++G(d,p) level were subsequently carried out. The frequency calculation, zero-point energy (ZPE) correction, and thermal energy correction for Gibbs free energy were performed at the same level of theory

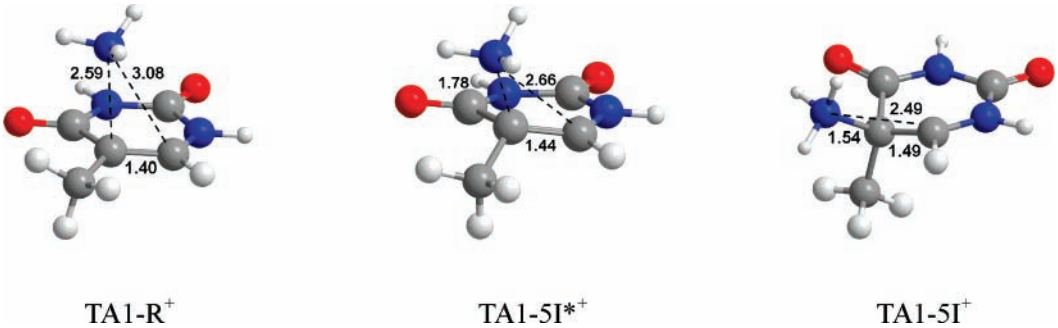

Figure 3. Optimized structures of solvated thymine radical cations with one ammonia molecule at the local minima or transition states along the reaction coordinate of the nucleophilic addition to the C5-site of Thy^+.

TABLE 1: Thermodynamic Properties of Thymine Radical Cations Solvated with One and Two Ammonia Molecules in the Gas Phase and in Aqueous Solution[a]

	ΔE_0[b]	ΔS_{298}[c]	ΔG_{298}[d]	ΔG_{solv}[e]	ΔG_{sol}[f]
TA2-R^+	0	0.13	0	−63.10	0
TA2-$5I^+$	−2.49	0.11	−0.31	−68.22	−5.43
TA2-$5P^+$	−4.30	0.11	−1.06	−70.52	−8.48
TA2-$6I^+$	−0.54	0.12	0.61	−77.99	−14.28
TA2-$6P^+$	−2.24	0.11	0.73	−75.98	−12.15
TA2-$5I^{*+}$	1.29	0.12	2.83	−64.63	1.30
TA2-$5P^{*+}$	−2.24	0.11	1.04	−70.23	−6.09
TA2-$6I^{*+}$	2.51	0.12	3.39	−64.77	1.72
TA2-$6P^{*+}$	−0.49	0.11	1.98	−76.61	−11.53
TA1-R^+	0	0.11	0	−68.19	0
TA1-$5I^+$	5.95	0.10	7.87	−76.31	−0.25
TA1-$5I^{*+}$	6.29	0.10	8.03	−74.32	1.90

[a] Energy in kcal/mol. [b] Relative energy at 0 K in the gas phase with ZPE correction. [c] Entropy (kcal/mol·K) in the gas phase at 298.15 K. [d] Relative free energy in the gas phase. [e] Solvation free energy calculated at the B3LYP/6-311++G(d,p) level using CPCM−UAKS. [f] Relative free energy in aqueous solution.

with the scaling factor of 0.978.[21] No imaginary vibrational frequencies were found for all of the local minimum structures, and only one imaginary frequency was shown for the transition states.

The spin and electron density distributions as well as the coefficients of a singly occupied molecular orbital (SOMO) and a lowest unoccupied molecular orbital (LUMO) for thymine radical cations solvated with ammonia molecules were calculated at the B3LYP/6-311++G(d,p) level using the optimized geometries. The spin density distribution of the neutral triplet of thymine was estimated at the same level of theory with the optimized geometry of thymine radical cation. These spin density analyses have been carried out to estimate the reactivity in various radical systems.[22−25] We employed Mulliken population analyses which are believed to be reliable for our system since the coefficients of SOMO for C5 and C6 of thymine radical cations solvated with ammonia molecules show a consistent trend with the Mulliken spin densities. Actually, Mulliken spin density analyses have been successfully used to predict the reactivity of the radical-involved reactions.[23,24]

Solvation free energies (ΔG_{solv}) of the optimized gas-phase structures were estimated by single-point calculations at the B3LYP/6-311++G(d,p) level with the UAKS cavities using the conductor-like polarizable continuum model (CPCM).[26] The spin and electron density distributions and the orbital coefficients of SOMO and LUMO in aqueous solution were also estimated at the same level of theory using CPCM−UAKS.

The spin-unrestricted calculations (UB3LYP) were used for all of the radicals and the radical cations. In these calculations, the expectation values of $\langle S^2 \rangle$ for the doublet systems ranged from 0.755 to 0.760. All calculations were carried out using the GAUSSIAN 03 package.[27]

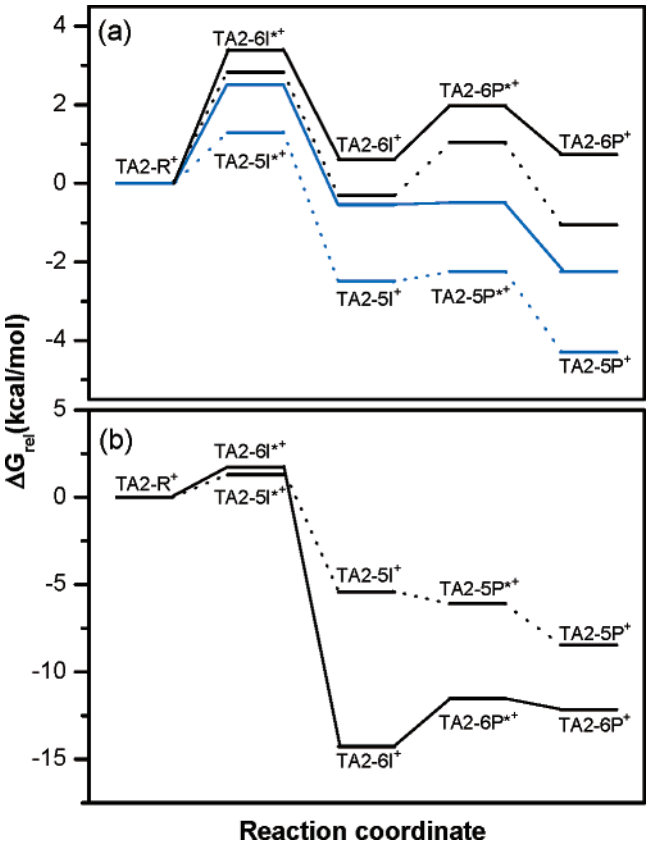

Figure 4. Energy diagram of the relative free energies at 0 K (blue) and 298.15 K (black) for solvated thymine radical cations with two ammonia molecules (a) in the gas phase and (b) in aqueous solution along the reaction coordinate of the nucleophilic addition to the C5-(dotted line) and C6-sites (solid line) of Thy^+.

Results and Discussion

Thymine radical cations solvated with a few number of water or ammonia molecules were used as models to explore the nucleophilic addition reaction to the C5−C6 double bond of Thy^+ in the gas phase as well as in aqueous solution.

Addition of Water. The OH^- addition product of the thymine radical cation may result literally from the addition of OH^-. However, due to the extremely low concentration of OH^- in aqueous solution, water is more likely to be the nucleophile for the reaction.[28] Scheme 1 depicts the water addition to Thy^+ leading to the C5−OH (**1**) or the C6−OH (**2**) radical, which could convert to the hydroperoxides or oxidation products in subsequent reactions with oxygen molecules.[10,11]

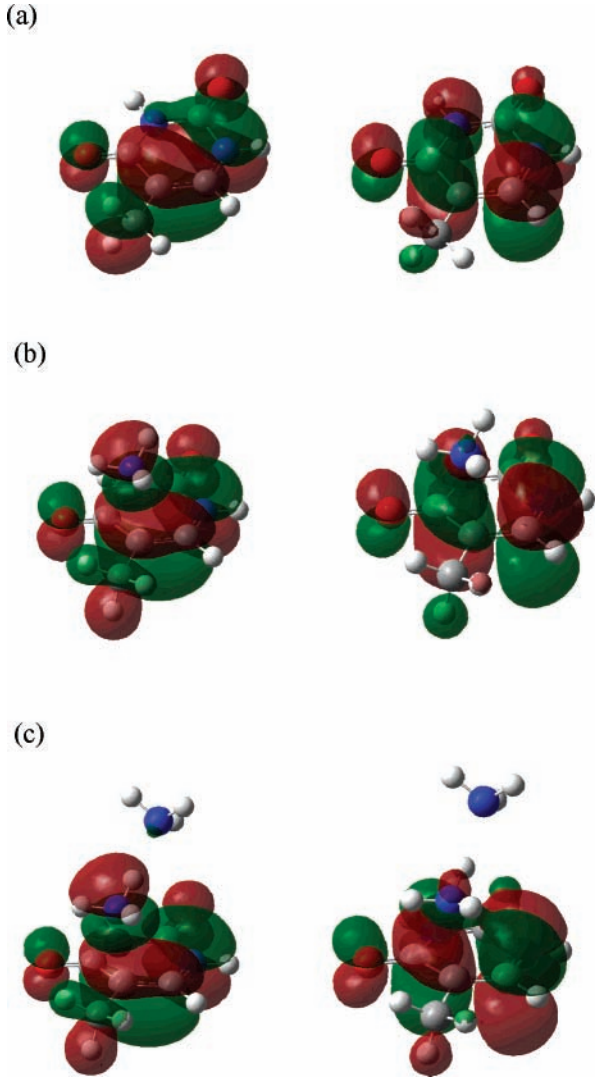

Figure 5. Pictorial representations of SOMO (left) and LUMO (right) for (a) Thy^+, (b) TA1-R^+, and (c) TA2-R^+. Each orbital is displayed with translucent orbital outlines.

The enthalpies of the reactions at 298.15 K in Scheme 1 were calculated using CPCM−UAKS at the HF/6-31+G(d)//HF/6-31+G(d) level. They were −13.2 and −24.9 kcal/mol for the formation of the C5−OH and the C6−OH radical in aqueous solution, respectively, with the enthalpy of hydration for a proton (−274.9 kcal/mol).[29] These results support the experimental observations that the dominant product of the water addition was the C6−OH radical in bulk solution.[20]

However, in our calculation, when we added a water molecule to the C6-site of Thy^+ in the gas phase, no covalent bond was formed between the water and the C6. In the relaxed potential energy scan, we found that the energy kept increasing without any stationary point as the water molecule got closer to the C6. This was also true with two water molecules added as a cluster, where the second water molecule played a role as the acceptor of a proton generated in the nucleophilic addition reaction.

On the contrary, however, when a water molecule was added to the C5-site, it easily formed a covalent bond with the C5. In this reaction, the proton was immediately released from a water molecule and attached to the O8 without forming an intermediate adduct of $[Thy/H_2O]^+$.

These results are quite opposite to the previous experimental observations in bulk solution where the water addition preferred the C6-site. Based on these results, we expect that the main product of water addition reaction with thymine radical cation would be C5−OH in gas phase, and the solvation effect in bulk solution would reverse this preference, leading to the formation of C6 adduct.

TABLE 2: Spin Density and Charge Density Distributions of Ammoniated Thymine Radical Cations and the Neutral Triplet State of Thymine in the Gas Phase

	T^+		^3T	$T^+(NH_3)_1$		$T^+(NH_3)_2$	
	spin	charge	spin	spin	charge	spin	charge
N1	0.283	−0.261	0.214	0.195	−0.321	0.155	−0.287
C2	−0.041	0.334	0.006	−0.025	0.289	−0.015	0.221
N3	−0.013	−0.356	0.042	−0.015	−0.376	−0.013	−0.335
C4	−0.080	0.160	0.013	−0.011	0.039	0.018	−0.028
C5	0.534	0.495	0.764	0.330	0.061	0.178	−0.023
C6	0.041	−0.131	0.690	0.157	0.103	0.255	−0.013
O7	0.108	−0.173	0.073	0.084	−0.204	0.073	−0.219
O8	0.120	−0.175	0.208	0.071	−0.207	0.046	−0.209
C11	−0.018	−0.671	−0.008	−0.017	−0.341	−0.029	−0.226

Addition of Ammonia. To see whether the preference for the C5-addition is unique for the water case, we investigated the structures and energies of thymine radical cations undergoing the nucleophilic addition by ammonia molecules (Scheme 2). Ammonia was chosen because it is a stronger nucleophile than water[30] and hence expected to be able to form a covalent bond even on the C6-site with the smaller number of ammonia molecules. This was necessary in order to follow both the C5- and C6-addition reactions with a limited CPU time and hence to investigate the selectivity between C5- and C6-sites of thymine radical cation for the nucleophilic addition reaction. Indeed, different from the case with water, the addition of two ammonia molecules as a cluster formed a covalent bond with the C6.

Figures 1 and 2 show the optimized structures of the solvated clusters of Thy^+ with two ammonia molecules at the local minima or the transition states along the nucleophilic addition reactions to the C5- and C6-sites of Thy^+, respectively. As in the case of water addition, one ammonia molecule could not form a covalent bond with the C6. The local minimum and transition state structures of the solvated Thy^+ with one ammonia molecule along the addition reaction to the C5-atom is shown in Figure 3. The relative energies, entropies, and free energies of the optimized structures are also listed in Table 1. The energy diagram, which represents the relative free energies along the reaction coordinate, is shown in Figure 4a. The solvation free energies calculated for all of the local minima and transition states in Figures 1 and 2 are also included in Table 1. The relative free energies in aqueous solution were calculated with the solvation free energies and plotted along the reaction coordinate in Figure 4b.

The reaction coordinates were chosen along the lowest energy pathways connecting the reactant (TA2-R^+) to the products (TA2-5P^+ and TA2-6P^+) via the intermediate states (TA2-5I^+ and TA2-6I^+). The pathway from TA2-R^+ to TA2-5I^+ was obtained by adiabatically optimizing the structures along the distance between the nucleophile and C5 of Thy^+, which was varied from the value of the reactant to that of the intermediate with the interval of 0.1 Å. The transition state was located at the highest energy point along this pathway. In order to find the pathway to TA2-6I^+, a 2-D potential energy surface was constructed by the adiabatic optimizations with both distances from the nucleophile to the C5 and to the C6 as the frozen coordinates, which were varied from the values of the reactant to those of the intermediate. The lowest energy pathways from the intermediates to the products were also obtained by

TABLE 3: SOMO and LUMO Coefficients of Ammoniated Thymine Radical Cations in the Gas Phase

	T^+				$T^+(NH_3)_1$				$T^+(NH_3)_2$			
	SOMO		LUMO		SOMO		LUMO		SOMO		LUMO	
	$2p_z$	$3p_z$	$2p_z$	$3p_z$	$2p_z$	$3p_z$	$2p_z$	$3p_z$	$2p_z$	$3p_z$	$2p_z$	$3p_z$
C5	0.176	0.281	−0.134	−0.209	0.157	0.239	−0.136	−0.203	0.140	0.212	−0.134	−0.201
C6	0.098	0.158	0.211	0.331	0.111	0.176	0.192	0.298	0.113	0.177	0.165	0.255

adiabatically optimizing the structures along the N−H bond length of ammonia which was covalently bonded to Thy^+.

All of the local minimum and transition state structures along the reaction coordinate of the NH_3 addition to the C6-site have a higher energy than the corresponding structures along the reaction to the C5-site. The relative energies (ΔE_0) of the transition states for the formation of the intermediates, TA2-5I$^+$ and TA2-6I$^+$, in the gas phase were 1.29 and 2.51 kcal/mol, respectively, with respect to the energy of TA2-R$^+$. The relative energies of the C5−NH_2 and the C6−NH_2 radical product (TA2-5P$^+$ and TA2-6P$^+$) were −4.30 and −2.24 kcal/mol, respectively. These results indicate that the addition to the C5-site is more favorable than to the C6-site in the gas phase when two ammonia molecules were added as a cluster. This is also consistent with the results for the addition of one ammonia or water clusters where the addition occurs only to the C5-site.

In aqueous solution, however, most of the local minimum and transition state structures along the addition to the C6-site have a lower energy than the corresponding structures along the reaction to the C5-site. These coincide well with previous experimental observations for the addition of water that the dominant product was from the addition to the C6-site rather than to the C5. The only exception is the transition state for the formation of the intermediate, TA2-6I$^+$ (Figure 4b). The transition state of TA2-6I*$^+$ is slightly higher in energy than that of TA2-5I*$^+$.

In order to find out the factors governing the preferential attack on the C5-site of Thy^+ by a nucleophile in the gas phase, we calculated molecular orbital factors and estimated the relative reactivity of the C5 and the C6 by applying the valence bond configuration mixing (VBCM) model. Shaik[31] first proposed this model as an approach to reactivity of organic reactions and applied it to predict the regioselectivity of nucleophilic attack on radical cations. They suggested that the regiochemical pathway prefers the nucleophilic attack at the position with the highest orbital coefficient in the LUMO of the radical cation and also with the highest spin density of the corresponding neutral parent in the triplet state.[32] Herbertz et al.[23] also suggested the importance of the SOMO orbital coefficients in predicting the reactivity of the radical cation of a bridged norcaradiene toward a nucleophile.

The spin and charge density distributions of Thy^+, TA1-R$^+$, and TA2-R$^+$ and the triplet spin densities of neutral thymine are listed in Table 2. TA1-R$^+$ and TA2-R$^+$ were chosen because they were most likely to be the geometries of the reactants for the ammonia addition among other fully optimized structures of the solvated cluster ions. In TA1-R$^+$ and TA2-R$^+$, the ammonia molecules are closer to the C5 than the C6. The distances from the C5 and the C6 to the N-atom of the closest ammonia are 2.59 and 3.08 Å for TA1-R$^+$, and those for TA2-R$^+$ are 2.39 and 2.95 Å, respectively.

For the triplet spin density of the neutral thymine (^{3}T), the spin density of the C5 (0.764) is slightly higher than that of the C6 (0.690). The spin density distributions also show that the C5 has the higher density than the C6 when the ammonia molecule either is completely separated from the Thy^+ or approaches it for the reaction (it corresponds to TA1-R$^+$ case).

TABLE 4: Spin and Charge Density Distributions of Ammoniated Thymine Radical Cations and the Neutral Triplet State of Thymine in Aqueous Solution Calculated at the B3LYP/6-311++G(d,p) Level Using CPCM−UAKS

	T^+		^{3}T	$T^+(NH_3)_1$		$T^+(NH_3)_2$	
	spin	charge	spin	spin	charge	spin	charge
C5	0.574	0.671	0.733	0.321	0.242	0.172	0.111
C6	0.003	−0.193	0.660	0.137	0.012	0.230	−0.055

In TA2-R$^+$, the spin density of the C6 becomes larger than that of the C5. Obviously, the orbital coefficients of the SOMO for Thy^+, TA1-R$^+$, and TA2-R$^+$ show a similar trend although the coefficient of C5 is still larger than that of C6 even in TA2-R$^+$ with the marginal difference. The SOMO and LUMO of the three radical cations are shown in Figure 5, and the coefficients for the $2p_z$ and $3p_z$ orbitals of the C5 and C6 are listed in Table 3.

The orbital coefficients of the SOMO and LUMO are large at N1, C5, and C6 for all of the three radical cations. For the SOMO, the largest orbital coefficient is at C5. However, the difference in the coefficient between the C5 and C6 gets smaller as it goes from Thy^+ to TA2-R$^+$. On the other hand, the largest orbital coefficient of the LUMO is at C6. However, as the case of the SOMO, the difference between the C6 and C5 becomes smaller as the number of ammonia molecules in the radical cations increase.

With the higher triplet spin density of the C5 than that of the C6, the VBCM model predicts that the nucleophilic addition is more favorable toward the C5 than the C6 for Thy^+. The larger orbital coefficient of the SOMO, which must be involved in the reaction, also makes the C5 more reactive. These explain our theoretical results that the single ammonia molecule can form a covalent bond with the C5 of Thy^+, but not with the C6.

The difference in the orbital coefficient between the C5 and C6, however, becomes smaller as the number of ammonia molecules in the cluster ions increases. This also agrees well with our calculation results on TA2-R$^+$. Different from the case of TA1-R$^+$, both the C5- and the C6-atom of TA2-R$^+$ form a covalent bond with the ammonia molecule, though the formation of the C5−NH_3 adduct is still more favorable.

The variations on the SOMO coefficients with the number of ammonia molecules in the cluster ions can be due to the change in local environments near the C5 and the C6 by the ammonia molecules. With partially negative charge density on the N-atom of ammonia, it approaches toward the C5 of the highest positive charge density and forms a stable complex with Thy^+ at the distances of 2.59 and 2.39 Å for TA1-R$^+$ and TA2-R$^+$, respectively. This may in turn give rise to large electron−electron repulsion between the N-atom of ammonia and the C5, which results in the transfer of some of the spin density from the C5 to the C6. When two ammonia molecules approach as a dimer to the C5, the repulsion would become larger with the shorter distance between the N-atom and the C5 compared to the case with a single ammonia molecule. This may cause the transfer of even larger amount of the spin density from the C5 to the C6.

Note that the higher reactivity of the C5 than that of the C6 of Thy^+ toward the nucleophilic addition could not be predicted

TABLE 5: SOMO and LUMO Coefficients of Ammoniated Thymine Radical Cations in Aqueous Solution Calculated at the B3LYP/6-311++G(d,p) Level Using CPCM−UAKS

	T^+				$T^+(NH_3)_1$				$T^+(NH_3)_2$			
	SOMO		LUMO		SOMO		LUMO		SOMO		LUMO	
	$2p_z$	$3p_z$	$2p_z$	$3p_z$	$2p_z$	$3p_z$	$2p_z$	$3p_z$	$2p_z$	$3p_z$	$2p_z$	$3p_z$
C5	0.183	0.295	−0.117	−0.185	0.161	0.246	−0.119	−0.180	0.145	0.219	−0.118	−0.177
C6	0.090	0.145	0.210	0.331	0.104	0.165	0.191	0.299	0.107	0.169	0.165	0.256

with the orbital coefficients of the LUMO. The same situation was reported by Glatthar et al.[33] They could not predict the preferential formation of the nucleophilic addition product of the intermediate DNA radical cations with the LUMO coefficients, though they could with the triplet spin density of the corresponding neutral molecules. These may be due to the relative importance of the triplet spin density compared to the LUMO coefficient in determining the regioselectivity of nucleophilic addition reactions toward radical cations. In other words, the factor associated with the high spin density in the VBCM model (denoted as f_0) played more dominant role in determining the height of the reaction barrier than that with the large LUMO coefficient (denoted as B) in these systems.[31]

To investigate the solvent effects on the relative reactivity of the C5 and C6 of Thy^+, the same analyses were performed for Thy^+, TA1-R^+, TA2-R^+, and the neutral triplet of thymine in aqueous solution using CPCM−UAKS. The spin and charge density distributions in aqueous solution are listed in Table 4. The SOMO and LUMO coefficients for the $2p_z$ and $3p_z$ orbitals of the C5 and C6-atoms are listed in Table 5. Consistent with the gas-phase results, the triplet spin density of the C5 of neutral thymine (^3T) in aqueous solution is still higher than that of the C6, although the difference is small. The SOMO orbital coefficients of the C5 are also higher than those of the C6 for Thy^+, TA1-R^+, and TA2-R^+ in aqueous solution. These indicate that the nucleophile is more likely to attack the C5 rather than the C6 of Thy^+ even in aqueous solution. The higher reactivity of the C5 than that of the C6 for the nucleophilic addition is also represented in the energy diagram of the reaction (Figure 4b). The transition state of forming TA2-$5I^+$ has the lower energy than that of forming TA2-$6I^+$, though TA2-$6I^+$ becomes much more stable in aqueous solution than TA2-$5I^+$ by solvation. Therefore, we suggest that the nucleophilic addition to the C6-site is thermodynamically favored in aqueous solution, whereas that to the C5-site is kinetically favored.

Conclusions

DFT studies to investigate the reactivity between C5 and C6 in the nucleophilic addition reaction of water and ammonia to Thy^+ were presented. The preferential attack of the nucleophile was predicted to occur on the C5-site rather than on the C6-site of Thy^+ in the gas phase. The C6 does not form a covalent bond with either one or two water molecules. With ammonia molecule as a stronger nucleophile than water, we could observe the decrease of selectivity in the nucleophilic attack on the C5-site over the C6-site with the number of nucleophile molecules, which was attributed to the intramolecular electron density redistribution within Thy^+ induced by the ammonia molecules.

Little effect of solvation by water was predicted on the molecular orbital factors that may govern the reactivity of the C5- and C6-sites of Thy^+. This agrees well with the calculation results that the transition state of forming the C5−NH_3 adduct has a slightly lower energy than that of forming the C6−NH_3 in aqueous solution, in spite of the significantly higher energy of the C5−NH_3 than the C6−NH_3. Therefore, extending this idea to the case of water addition we suggest that the observed dominance of the C6−OH radical product in bulk solution is not because the C6-site becomes more favorable for the nucleophilic addition than the C5 in solution, but because the C6−OH radical product as well as the C6−OH_2 intermediate become much more stable in solution compared with the C5−OH and C5−OH_2, respectively.

This study supports that DFT methods can be used to construct the reliable potential energy surface for the reactions of the radicals derived from DNA bases, showing that they could be further utilized for other interesting biological systems.

Acknowledgment. This work was supported by the research grant of the Chungbuk National University in 2006. N.J.K. thanks Professor Young Kee Kang for helpful discussions.

Supporting Information Available: Optimized geometries of the structures in Figures 1−3. This material is available free of charge via the Internet at http://pubs.acs.org.

References and Notes

(1) Von Sonntag, C. *Free-Radical-Induced DNA Damage and Its Repair*; Springer-Verlag: Berlin, 2006.
(2) Yan, M.; Becker, D.; Summerfield, S.; Renke, P.; Sevilla, M. D. *J. Phys. Chem.* **1992**, *96*, 1983.
(3) Little, J. B. *Carcinogenesis* **2000**, *21*, 397.
(4) Hwang, C. T.; Stumpf, C. L.; Yu, Y.-Q.; Kenttamaa, H. I. *Int. J. Mass Spectrom.* **1999**, *182/183*, 253.
(5) Steenken, S. *Chem. Rev.* **1989**, *89*, 503.
(6) Close, D. M. *J. Phys. Chem. B* **2003**, *107*, 864.
(7) Kobayashi, K.; Tagawa, S. *J. Am. Chem. Soc.* **2003**, *125*, 10213.
(8) Price, J. M.; Petzold, C. J.; Byrd, H. C. M.; Kenttamaa, H. I. *Int. J. Mass Spectrom.* **2001**, *212*, 455.
(9) Wetmore, S. D.; Himo, F.; Boyd, R. J.; Eriksson, L. A. *J. Phys. Chem. B* **1998**, *102*, 7484.
(10) Wagner, J. R.; van Lier, J. E.; Johnston, L. J. *Photochem. Photobiol.* **1990**, *52*, 333.
(11) Sevilla, M. D. *J. Phys. Chem.* **1971**, *75*, 626.
(12) Sevilla, M. D.; Van Paemel, C.; Zorman, G. *J. Phys. Chem.* **1972**, *76*, 3577.
(13) Steenken, S. *Free Radical Res. Commun.* **1992**, *16*, 349.
(14) Deeble, D. J.; Schuchmann, M. N.; Steenken, S.; von Sonntag, C. *J. Phys. Chem.* **1990**, *94*, 8186.
(15) Close, D. M. *Radiat. Res.* **1993**, *135*, 1.
(16) Lomoth, R.; Brede, O. *Chem. Phys. Lett.* **1998**, *288*, 47.
(17) Geimer, J.; Brede, O.; Beckert, D. *Chem. Phys. Lett.* **1997**, *276*, 411.
(18) Sevilla, M. D.; Engelhardt, M. L. *Faraday Discuss. Chem. Soc.* **1977**, *63*, 255.
(19) Shaw, A. A.; Voituriez, L.; Cadet, J.; Gregoli, S.; Symons, M. C. R. *J. Chem. Soc., Perkin Trans. 2* **1988**, 303.
(20) Geimer, J.; Beckert, D. *J. Phys. Chem. A* **1999**, *103*, 3991.
(21) Kang, Y. K. *J. Mol. Struct. (THEOCHEM)* **2001**, *546*, 183.
(22) Mitrasinovic, P. M. *Bioconjugate Chem.* **2005**, *16*, 588.
(23) Herbertz, T.; Blume, F.; Roth, H. D. *J. Am. Chem. Soc.* **1998**, *120*, 4591.
(24) Grapperhaus, C. A.; Kozlowski, P. M.; Kumar, D.; Frye, H. N.; Venna, K. B.; Poturovic, S. *Angew. Chem., Int. Ed.* **2007**, *46*, 4085.
(25) Ban, F.; Lundqvist, M. J.; Boyd, R. J.; Eriksson, L. A. *J. Am. Chem. Soc.* **2002**, *124*, 2753.
(26) Takano, Y.; Houk, K. N. *J. Chem. Theory Comput.* **2005**, *1*, 70.
(27) Frisch, M. J.; Trucks, G. W.; Schlegel, H. B.; Scuseria, G. E.; Robb, M. A.; Cheeseman, J. R.; Montgomery, J. A., Jr.; Vreven, T.; Kudin, K. N.; Burant, J. C.; Millam, J. M.; Iyengar, S. S.; Tomasi, J.; Barone, V.; Mennucci, B.; Cossi, M.; Scalmani, G.; Rega, N.; Petersson, G. A.; Nakatsuji, H.; Hada, M.; Ehara, M.; Toyota, K.; Fukuda, R.; Hasegawa, J.;

Ishida, M.; Nakajima, T.; Honda, Y.; Kitao, O.; Nakai, H.; Klene, M.; Li, X.; Knox, J. E.; Hratchian, H. P.; Cross, J. B.; Adamo, C.; Jaramillo, J.; Gomperts, R.; Stratmann, R. E.; Yazyev, O.; Austin, A. J.; Cammi, R.; Pomelli, C.; Ochterski, J. W.; Ayala, P. Y.; Morokuma, K.; Voth, G. A.; Salvador, P.; Dannenberg, J. J.; Zakrzewski, V. G.; Dapprich, S.; Daniels, A. D.; Strain, M. C.; Farkas, O.; Malick, D. K.; Rabuck, A. D.; Raghavachari, K.; Foresman, J. B.; Ortiz, J. V.; Cui, Q.; Baboul, A. G.; Clifford, S.; Cioslowski, J.; Stefanov, B. B.; Liu, G.; Liashenko, A.; Piskorz, P.; Komaromi, I.; Martin, R. L.; Fox, D. J.; Keith, T.; Al-Laham, M. A.; Peng, C. Y.; Nanayakkara, A.; Challacombe, M.; Gill, P. M. W.; Johnson, B.; Chen, W.; Wong, M. W.; Gonzalez, C.; Pople, J. A. *Gaussian 03*, revision C.02; Gaussian, Inc.: Wallingford, CT, 2004.

(28) Reynisson, J.; Steenken, S. *Phys. Chem. Chem. Phys.* **2002**, *4*, 527.

(29) Tissandier, M. D.; Cowen, K. A.; Feng, W. Y.; Gundlach, E.; Cohen, M. H.; Earhart, A. D.; Coe, J. V.; Tuttle, T. R., Jr. *J. Phys. Chem. A* **1998**, *102*, 7787.

(30) Mohr, M.; Zipse, H. *Phys. Chem. Chem. Phys.* **2001**, *3*, 1246.

(31) (a) Shaik, S. *J. Am. Chem. Soc.* **1981**, *103*, 3692. (b) Shaik, S.; Shurki, A. *Angew. Chem., Int. Ed.* **1999**, *38*, 586.

(32) Eberson, L.; Gonzalez-Luque, R.; Merchan, M.; Radner, F.; Roos, B. O.; Shaik, S. *J. Chem. Soc., Perkin Trans. 2* **1997**, 463.

(33) Glatthar, R.; Spichty, M.; Gugger, A.; Batra, R.; Damm, W.; Mohr, M.; Zipse, H.; Giese, B. *Tetrahedron* **2000**, *56*, 4117.